DIELECTRONIC RECOMBINATION OF Fe XIX FORMING Fe XVIII: LABORATORY MEASUREMENTS AND THEORETICAL CALCULATIONS

D. W. Savin and S. M. Kahn

Columbia Astrophysics Laboratory and Department of Physics, Columbia University, New York, NY 10027; savin@astro.columbia.edu

J. Linkemann, A. A. Saghiri, M. Schmitt, M. Grieser, R. Repnow, D. Schwalm, and A. Wolf

Max-Planck-Institut für Kernphysik, D-69117 Heidelberg, Germany; and Physikalisches Institut der Universität Heidelberg, D-69120 Heidelberg, Germany

T. Bartsch, A. Müller, and S. Schippers

Institut für Kernphysik, Strahlenzentrum der Justus-Liebig-Universität, D-35392 Giessen, Germany

M. H. Chen

Lawrence Livermore National Laboratory, Livermore, CA 94550

N. R. Badnell

Department of Physics and Applied Physics, University of Strathclyde, Glasgow, G4 0NG, UK

and

T. W. Gorczyca and O. Zatsarinny

Department of Physics, Western Michigan University, Kalamazoo, MI 49008

ABSTRACT

We have measured resonance strengths and energies for dielectronic recombination (DR) of Fe XIX forming Fe XVIII via $N = 2 \rightarrow N' = 2$ and $N = 2 \rightarrow N' = 3$ core excitations. All measurements were carried out using the heavy-ion Test Storage Ring at the Max Planck Institute for Nuclear Physics in Heidelberg, Germany. We have also calculated these resonance strengths and energies using two independent, state-of-the-art techniques: the perturbative multiconfiguration Breit-Pauli (MCBP) and multiconfiguration Dirac-Fock (MCDF) methods. Overall, reasonable agreement is found between our experimental results and theoretical calculations. The most notable discrepancies are for the $3l3l'$ resonances. The calculated MCBP and MCDF resonance strengths for the $n = 3$ complex lie, respectively, $\approx 47\%$ and $\approx 31\%$ above the measured values. These discrepancies are larger than the estimated $\lesssim 20\%$ total experimental uncertainty in our measurements. We have used our measured $2 \rightarrow 2$ and $2 \rightarrow 3$ results to produce a Maxwellian-averaged rate coefficient for DR of Fe XIX. Our experimentally derived rate coefficient is estimated to be good to better than $\approx 20\%$ for $k_B T_e \geq 1$ eV. Fe XIX is predicted to form in photoionized and collisionally ionized cosmic plasmas at $k_B T_e \gg 1$ eV. Hence, our rate coefficient is suitable for use in ionization balance calculations of these plasmas. Previously published theoretical DR rate coefficients are in poor agreement with our experimental results. None of these published calculations reliably reproduce the magnitude or temperature dependence of the experimentally derived rate coefficient. Our MCBP and MCDF results agree with our experimental rate coefficient to within $\approx 20\%$.

Subject heading: atomic data — atomic processes — methods: laboratory

1. INTRODUCTION

Dielectronic recombination (DR) is the dominant electron-ion recombination mechanism for most ions in both photoionized and electron-ionized cosmic plasmas (Ferland et al. 1998; Mazzotta et al. 1998). Interpreting and modeling the line emission and thermal and ionization structures of these plasmas require reliable DR rate coefficients (Mewe, Gronenschild, & van den Oord 1985; Brickhouse, Raymond, & Smith 1995; Ferland et al. 1998; Müller 1999; Savin et al. 1999, 2000). Theoretical calculations are used for essentially all the required DR rate coefficients (Kallman & Bautista 2001; Ferland et al. 1998; Mazzotta et al. 1998). However, for L- and M-shell ions where DR measurements exist, experiments have found factor of 2 to order-of-magnitude errors in the published theoretical DR rate coefficients (Linkemann et al. 1995; Savin et al. 1997, 1999, 2002; Müller 1999; Schippers et al. 1998, 2000, 2001), and for ions where no measurements exist, the various published

theoretical results for a given ion can differ by factors of 2 or more (Arnaud & Raymond 1992; Müller 1999; Savin 2000; Savin & Laming 2002). These uncertainties in the DR rate coefficients limit our ability to infer the properties of cosmic plasmas.

Of particular importance are the DR rate coefficients for the iron L-shell ions (Fe XVII to Fe XXIV). These ions are an important source of line emission in the extreme-UV to X-ray spectral range and have been detected in a wide range of solar and cosmic sources (Doschek & Cowan 1984; Mewe 1991; Lum et al. 1992; Dupree et al. 1993). The need for reliable L-shell iron DR rate coefficients has become particularly urgent since the launches of *Chandra* and *XMM-Newton*. These satellite observatories are collecting high-resolution X-ray spectra that are rich in emission from L-shell iron (see, e.g., Brinkman et al. 2000; Kaspi et al. 2000). Over the lifetime of their missions, these satellites are expected to observe L-shell line emission from hundreds of objects covering all classes of X-ray–emitting sources. Reli-
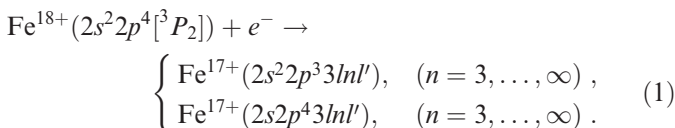
able DR rate coefficients will be needed to aid in interpreting these collected spectra.

In an attempt to prioritize the needed DR data for L-shell ions, Savin & Laming (2002) have investigated how uncertainties in the theoretical DR rate coefficients affect upper atmosphere abundance determinations for solar and stellar atmospheres. They found that of all the L-shell isoelectronic sequences, DR of oxygen-like ions forming fluorine-like ions was the highest priority system. Here we present experimental results for DR of oxygen-like Fe XIX forming Fe XVIII. We also present theoretical results using two independent theoretical techniques. Our laboratory measurements provide an important benchmark for these calculations, which can then be used to calculate other needed DR rate coefficients along the oxygen-like isoelectronic sequence.

DR is a two-step recombination process that begins when an electron collides with an ion, excites a bound electron of the ion, and is simultaneously captured by the ion. The excitation process can be written as $Nl_j \to N'l''_{j'}$, where N is the principal quantum number of the electron, l its orbital angular momentum, and j its total angular momentum. The total energy of this intermediate state lies in the continuum of the recombined ion, and the system may autoionize. DR occurs when the ion relaxes radiatively and emits a photon that reduces the total energy of the recombined ion to below its ionization threshold. DR can go forward when the center-of-mass collision energy (E_{cm}) and the binding energy released when the electron is captured (E_b) add up to the energy required to excite the core electron (ΔE). Because E_b and ΔE are quantized, DR is a resonant process.

In order to address the need for reliable L-shell iron DR rate coefficients, we have initiated a laboratory program of DR measurements on these systems. Experiments are carried out using the heavy-ion Test Storage Ring (TSR) at the Max Planck Institute for Nuclear Physics in Heidelberg, Germany (Müller & Wolf 1997). To date we have carried out $2 \to 2$ DR measurements at high electron energy resolution for Fe XVIII (Savin et al. 1997, 1999), Fe XIX (Savin et al. 1999), Fe XX (Savin et al. 2002), Fe XXI, Fe XXII, and Fe XXIV. Evaluation is currently underway for these latter three ionization stages. A preliminary overview of the $2 \to 2$ DR spectra acquired to date has been presented in Gwinner et al. (2001). Measurements (which preceded the present program) have also been carried out for $3 \to 3$, $2 \to 3$, and $2 \to 4$ DR of M-shell Fe XVI (Linkemann. 1995). We use the convention of identifying the recombination process by the initial charge state of the recombining ion and refer to the energy dependence of the DR cross section as the DR spectrum.

Here we present our results for $2 \to 2$ DR of Fe XIX for $E_{cm} \lesssim 0.066$ eV as well as for $2 \to 3$ DR of Fe XIX. Results for $2 \to 2$ DR resonances at $E_{cm} \gtrsim 0.066$ eV were presented by Savin et al. (1999). The relevant $2 \to 2$ DR capture channels are discussed in Savin et al. (1999). For $2 \to 3$ DR, we have carried out measurements of DR via the capture channels

$$\mathrm{Fe}^{18+}(2s^2 2p^4[^3P_2]) + e^- \to$$

$$\begin{cases} \mathrm{Fe}^{17+}(2s^2 2p^3 3lnl'), & (n = 3, \ldots, \infty), \\ \mathrm{Fe}^{17+}(2s 2p^4 3lnl'), & (n = 3, \ldots, \infty). \end{cases} \quad (1)$$

Dielectronic capture occurs for Fe XIX core excitations of

the type $2s^2 2p^3 3l$ and $2s 2p^4 3l$ for which experimental energy levels are available (Sugar & Corliss 1985). DR occurs when the resulting Fe XVIII ion radiatively stabilizes (generally to a $2s^2 2p^4 nl'$ system). This results in measurable DR resonances for 300 eV $\lesssim E_{cm} \lesssim 1000$ eV.

DR resonance energies can be predicted using the hydrogenic formula

$$E_{nl} = \Delta E - \left(\frac{z}{n - \mu_l}\right)^2 \mathcal{R} . \quad (2)$$

Here E_{nl} is the resonance energy for DR into a given nl level, z the charge of the ion before DR, μ_l the quantum defect for the recombined ion, and $\mathcal{R}$ the Rydberg energy. For DR into high-l levels, $\mu_l \approx 0$. Theoretically, the strongest resonance series are expected for those resonances corresponding to core excitations of the $2s^2 2p^3(^2D^o)3d(^3D^o_{J=1,2,3})$ levels since these levels have the strongest radiative rates. The $J = 3$ level is observed at $\Delta E = 917.0$ eV, while, theoretically, we estimate the $J = 1, 2$ levels to be at $\Delta E = 920.4$ eV and $\Delta E = 917.7$ eV, respectively. Other levels within $\approx \pm 15$ eV of 917 eV have smaller but still significant radiative rates, giving the measured DR resonances their apparent width.

Using the $2 \to 2$ results from Savin et al. (1999) along with our present $2 \to 2$ and $2 \to 3$, we are able to produce an experimentally derived, Maxwellian-averaged DR rate coefficient for Fe XIX. For ionization balance calculations, we have fitted our experimentally derived rate coefficient using a simple fitting formula. The resulting fit parameters are also presented here.

The paper is organized as follows: In § 2 we describe the experimental arrangement for the Fe XIX $2 \to 3$ DR measurements. The arrangement for the $2 \to 2$ results was discussed in Savin et al. (1999). We present our laboratory results in § 3. In § 4 we discuss published theoretical Fe XIX rate coefficients as well as several new theoretical calculations that we have carried out for comparison with our measurements. We compare our experimental results with tokamak measurements and theoretical results in § 5 and discuss our conclusions in § 6.

2. EXPERIMENTAL TECHNIQUE

The experimental arrangement for carrying out DR measurements at TSR is described in detail in Kilgus et al. (1992), Lampert et al. (1996), and Schippers et al. (1998, 2000, 2001). Details specific to our Fe XIX measurements can be found in Savin et al. (1999). Here we present only those aspects of the setup for the Fe XIX $2 \to 3$ DR measurements that were not discussed previously.

A 241 MeV beam of $^{56}\mathrm{Fe}^{18+}$ ions was injected into TSR and simultaneously cooled by a collinear electron beam. The electron beam acceleration voltage V_e was set to $V_{cool} \approx 2540$ V at injection/cooling, corresponding to matched ion and electron beam velocities. Approximately 1 s after injection, the acceleration voltage was increased to either $V_0 \approx 5000$ or ≈ 6050 V. The electron space charge reduced the electron beam energy with respect to eV_e in the interaction region by ≈ 120–260 eV. After the injection and the acceleration voltage jump from V_{cool} to V_0, a delay of ≈ 7 s allowed the various power supplies to stabilize before data acquisition. In addition, this delay was longer than the lifetime of any metastable Fe XIX ions (Cheng, Kim, &

Desclaux 1979), and the ions were assumed to be in their ground state for the DR measurements.

Data were collected by chopping the electron beam acceleration voltage between a reference value V_{ref}, a measurement value V_{meas}, and V_0. There was a delay of 5 ms at each voltage setting, adapted to the response time of the fast high-voltage supply used for this chopping, and then data were collected for 20 ms. The total data collection time with one fill of the ring was ≈ 30 s as the chopping pattern was repeated ≈ 400 times. With each repetition of the V_0-V_{ref}-V_{meas} scheme, the measurement voltage value V_{meas} was incremented by ≈ 0.5 V. At the end of the data acquisition, the acceleration voltage was reduced to $V_{cool} = 2540$ V and a new injection/cooling cycle begun.

At V_0 and during data acquisition, the ions were not being cooled by the electron beam. As a result, the ion beam expanded from an FWHM diameter of ≈ 2 mm at cooling to ≈ 6 mm. Measurements were carried out using stored ion currents of between ≈ 35 and 70 μA. The lifetime for the uncooled Fe XIX ions in TSR was ≈ 660 s. The electron beam density varied (depending on V_{meas}) between $\approx 2.2 \times 10^7$ and $\approx 4.1 \times 10^7$ cm^{-3} for the measurements reported here. The electron beam diameter was ≈ 3.4 cm.

Application of a space-charge correction (Kilgus et al. 1992) and a relativistic transformation from the laboratory frame of reference to the electron-ion center-of-mass frame transformed the voltages V_{meas} and V_{ref} into the center-of-mass energies E_{cm} and E_{ref}, respectively. The measured recombination signal rate was calculated by taking the rate at the measurement energy $R(E_{cm})$ and subtracting from it the corresponding rate at the reference energy $R(E_{ref})$. This eliminates the effects of slow pressure variations during the scanning of the measurement energy but not the effects of any fast pressure variations associated with the chopping of the electron beam energy, leaving a small residual charge transfer (CT) background. Following Schippers et al. (2000), the measured merged-beam rate coefficient $\alpha_L(E_{cm})$ is given by

$$\alpha_L(E_{cm}) = \frac{[R(E_{cm}) - R(E_{ref})]\gamma^2}{n_e N_i (L/C)\eta} + \alpha(E_{ref})\frac{n_e(E_{ref})}{n_e(E_{cm})} \ . \qquad (3)$$

Here N_i is the number of ions stored in the ring, $C = 55.4$ m the circumference of the ring, L the nominal length of the electron-ion overlap in the electron cooler, η the detection efficiency of the recombined ions (which is essentially 1), $\gamma^2 = [1 - (v/c)^2]^{-1} \approx 1.01$, and c the speed of light. The measured rate coefficient represents the DR and radiative recombination (RR) cross sections multiplied by the relative electron-ion velocity and then convolved with the experimental energy spread. The data sit on top of the residual CT background. The second term in equation (3) is a small correction to re-add the RR+DR signal at the reference that is subtracted out in the expression $[R(E_{cm}) - R(E_{ref})]$. The RR rate coefficient at E_{ref} is calculated using a modified semiclassical formula for the RR cross section (Schippers et al. 1998). Generally, E_{ref} is chosen so that the DR signal is small to negligible. When the DR signal at E_{ref} is small but nonnegligible, we use the theoretical DR rate coefficient. Using $\alpha_L(E_{cm})$, the effects of the merging and demerging of the electron and ion beams are accounted for, following the procedure described in Lampert et al. (1996), to produce a final measured recombination rate coefficient $\alpha(E_{cm})$ from which the DR results are extracted.

The first set of data was collected using $V_0 \approx 5000$ V and scanning V_{meas} from ≈ 4000 to ≈ 5860 V. After correcting for electron beam space-charge effects, this corresponds to scanning the electron-ion center-of-mass energies E_{cm} between ≈ 188 and ≈ 738 eV. Approximately 15 hr were required to cover this energy range. The reference voltage $V_{ref} \approx 4430$ V corresponds to a center-of-mass $E_{ref} \approx 274$ eV.

The second and third sets of data were collected using $V_0 \approx 6050$ V. For the second (third) data set, V_{meas} was scanned from ≈ 4950 (6140) to ≈ 6170 (6670) V. This corresponded to scanning E_{cm} between ≈ 477 (889) and ≈ 902 (1100) eV. Approximately 11 (2.5) hr were required to cover this energy range. The reference voltage used $V_{ref} \approx 6460$ (6650) V corresponds to an $E_{ref} \approx 931$ (1000) eV.

As discussed in Savin et al. (1999), small voltage errors resulted from the chopping of the electron beam acceleration voltage between V_{ref} and V_{meas}. For the $2 \rightarrow 3$ DR measurements, the relative influence on E_{cm} from this uncertainty is estimated to be less than 2%. We found that the peak energies in the overlapping energy regions of the first and second data sets differed by $\approx 1.5\%$ and for the overlapping regions of the second and third data sets by $\lesssim 0.5\%$. The observed energy differences can be explained on the basis of a later analysis of the voltage power supply system.

The three data sets were merged to produce a single data set. The DR peaks in the second data set occurred at center-of-mass energies ≈ 6.6 eV lower than the energies at which the corresponding peaks occurred in the first data set. The background in the second data set was slightly higher than the background in the first, by $\approx 1.4 \times 10^{-11}$ cm^3 s^{-1}. We adjusted the energy scale and background level of the second data set so that the data mapped smoothly onto the first data set. The DR series limit in the third data set occurred at an energy of ≈ 7.9 eV below the series limit in the corrected second data set. The background in the third data set matched that of the corrected second data set. We adjusted the energy scale of the third data set so that it mapped smoothly onto the corrected second data set. The resulting merged data set had a weak and slowly varying parabolic shape to the background level, which we fitted and subtracted out. This varying background level is attributed to fast pressure variations associated with the chopping of the electron beam energy.

To help verify the accuracy of the resulting experimental energy scale, we have used the prediction that the peak in the $2 \rightarrow 3$ DR resonances will be those associated with $2s^2 2p^3(^2D^o)3d(^3D^o_J)$ core excitations (spread across $\Delta E \approx 917.0$–920.4 eV). Using equation (2) and the measured resonance energies for the strongest peaks in the $3lnl'$ complexes for $n = 4, 5, 6$, and 7, we can extrapolate these data to $n = \infty$ to determine ΔE. The extrapolated value is 919.7 ± 0.8 eV. This agrees well with the expected range of values for ΔE. Taking everything into account, we conservatively estimate the overall systematic error of the merged experimental E_{cm} scale to be less than 2%.

As discussed in Savin et al. (1999), electrons captured into levels $n = n_{max} \gtrsim 130$ are field ionized in our experimental arrangement, and DR into levels above n_{max} is not detected. A detailed discussion of field ionization in TSR can be found in Schippers et al. (2001). The energy range affected by the field ionization of the recombined ions extends by ≈ 0.3 eV below each series limit (as given by the corresponding Fe XIX excitation energy). Because of the smallness of

the 0.3 eV energy range and the decrease of the DR cross section with increasing n, the influence of the suppressed high-Rydberg contribution on the thermal DR rate coefficient is negligible.

The background in the final measured rate coefficient $\alpha(E_{cm})$ was adjusted to match the theoretical RR rate coefficient over the measured energy range. The RR rate coefficient is small compared to DR in the energy range of 300–1000 eV. RR was calculated using a semiclassical hydrogenic cross section calculation (Schippers et al. 1998). As discussed in Kilgus et al. (1992), Lampert et al. (1996), and Savin et al. (1999), the total systematic uncertainty is estimated to be $\lesssim 20\%$. Relative uncertainties for comparing DR rate coefficients at large energy differences are estimated to be $\lesssim 10\%$. Uncertainties are quoted at a confidence level believed to be equivalent to a 90% counting statistics confidence level.

3. EXPERIMENTAL RESULTS

3.1. Near-Zero Energy $2 \rightarrow 2$ Resonances

Our results for those Fe XIX $2 \rightarrow 2$ DR resonances at $E_{cm} \gtrsim 0.066$ eV were presented in Savin et al. (1999). The lowest resonance at 0.066 eV was assigned to a blend of the $2s^2 2p^4(^3P_1)20l$ ($l \geq 3$) and $2s^2 2p^4(^3P_0)22p$ autoionizing levels, associated with fine-structure core excitations. Because of the energy spread of the electron beam, resonances at even lower energies cannot be resolved from the near 0 eV RR signal. However, we can infer the presence of such resonances. The measured recombination rate coefficient at $\lesssim 0.1$ eV is shown in Figure 1. The data represent the DR cross section σ times the relative electron-ion velocity v convolved with the energy spread of the experiment, a quantity we denote as the (merged beam) rate coefficient $\langle \sigma v \rangle$ and which is equivalent to $\alpha(E_{cm})$ defined in § 2. At $E_{cm} \lesssim 10^{-3}$ eV the measured rate coefficient is a factor of ≈ 10 times larger than the RR rate coefficient predicted using semiclassical RR theory with quantum mechanical corrections (Schippers et al. 1998). This enhancement factor is much larger than that found for Fe XVIII, for which the near 0 eV
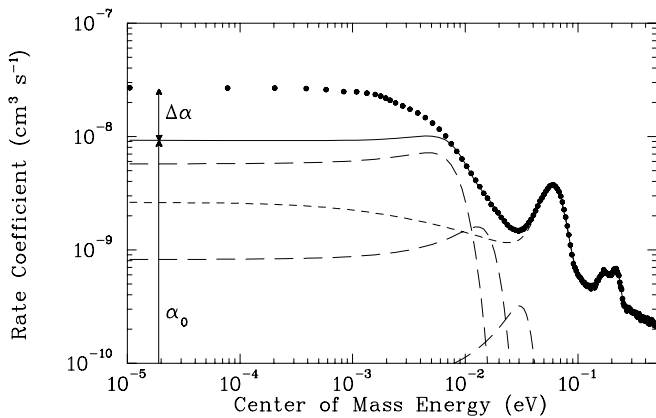

FIG. 1.—Measured and fitted Fe XIX to Fe XVIII $2 \rightarrow 2$ DR resonance structure below 0.5 eV. The experimental results are shown by the filled circles. The short-dashed curve is the fit to the data using our calculated RR coefficient and taking into account all resolved resonances. The solid curve is the fit α_0, which includes the estimated contributions from the unresolved $2s^2 2p^4(^3P_1)20d$ and $2s^2 2p^4(^3P_0)22s$ resonances (long-dashed curves; see § 3). At $E_{cm} = 10^{-5}$ eV, the difference between model spectrum α_0 and the data was adjusted so that $1 + \Delta\alpha/\alpha_0 = 2.9$.

recombination rate coefficient was a factor of ≈ 2.9 times larger than the theoretical RR rate coefficient. Fe XVIII is predicted to have no DR resonances near 0 eV, and we attribute this enhancement entirely to the still unresolved physics of electron-ion recombination at $E_{cm} \lesssim k_B T_e$ in electron coolers (Hoffknecht et al. 1998; Schippers et al. 1998; Gwinner et al. 2000; Hoffknecht et al. 2001). It is highly unlikely that the resolution of this issue will lead to a near 0 eV recombination rate coefficient that increases by a factor of ≈ 3 for a change in ionic charge from 17 to 18. Thus, we infer that there are unresolved DR resonances lying at energies below 0.066 eV.

Our calculations suggest that these unresolved resonances are due to a combination of the $2s^2 2p^4(^3P_1)20d$ and $2s^2 2p^4(^3P_0)22s$ configurations. Theoretical results indicate that these resonances have natural line widths significantly smaller than the energy spread of the experiment for the $2 \rightarrow 2$ measurements. Here we treat them as delta functions for fitting purposes. We find that if we assume a minimum of three resonances in calculating the model rate coefficient α_0, we can match the expected enhancement factor of $1 + \Delta\alpha/\alpha_0 = 2.9$ (see Fig. 1). The energies of the resonances that yield the best fit to the data at ~ 0.008–0.05 eV are 0.0087, 0.0180, and 0.0370 eV. The resonance strengths are, respectively, 29,000, 5000, and 800 in units of 10^{-21} cm^2 eV. The resulting model recombination spectrum below $E_{cm} = 0.5$ eV is presented in Figure 1. For the model spectrum, we use our inferred resonance strengths and energies as well as the extracted resonance strengths and energies of Savin et al. (1999).

3.2. $2 \rightarrow 3$ Resonances

The measured DR resonance structure for $2 \rightarrow 3$ DR onto Fe XIX is shown in Figure 2a. The spectrum is rich in resonance structure with many overlapping resonances within each manifold and between manifolds. The $3l3l'$, $3l4l'$, and $3l5l'$ manifolds are well separated in energy and easily identified. The higher $3lnl'$ ($n \geq 6$) manifolds are overlapping and less easily identifiable. However, we associate the strongest peak in each manifold with $2s^2 2p^3(^2D^o)3d(^3D^o_{J=1,2,3})$ excitations of Fe XIX as discussed in § 1. The energy resolution of the DR measurements can be approximated by a Gaussian with an FWHM of

$$\Delta E_{FWHM} = 4(k_B T_{eff} E_{cm} \ln 2)^{1/2}, \qquad (4)$$

where k_B is Boltzmann's constant and $k_B T_{eff}$ is the effective energy spread due to the combined energy spreads of the electron and ion beams. Because of blending of the DR resonances, we were unable to fit an individual DR resonance to determine the effective energy spread of the measurement. Instead we estimated the energy spread using our theoretical results convolved with Voigt profiles. The Voigt functions account for the Lorentzian natural line shapes of the resonances and the Gaussian shape of the experimental energy spread. We found a best fit by eye of $k_B T_{eff} \approx 1.125$ meV.

3.3. Rate Coefficients

Using the measured $2 \rightarrow 2$ resonance strengths and energies from Savin et al. (1999) and our inferred results for the near 0 eV resonances, we can produce a $2 \rightarrow 2$ DR rate coefficient for ions in a plasma with a Maxwellian electron energy distribution T_e. The technique for this straightfor-
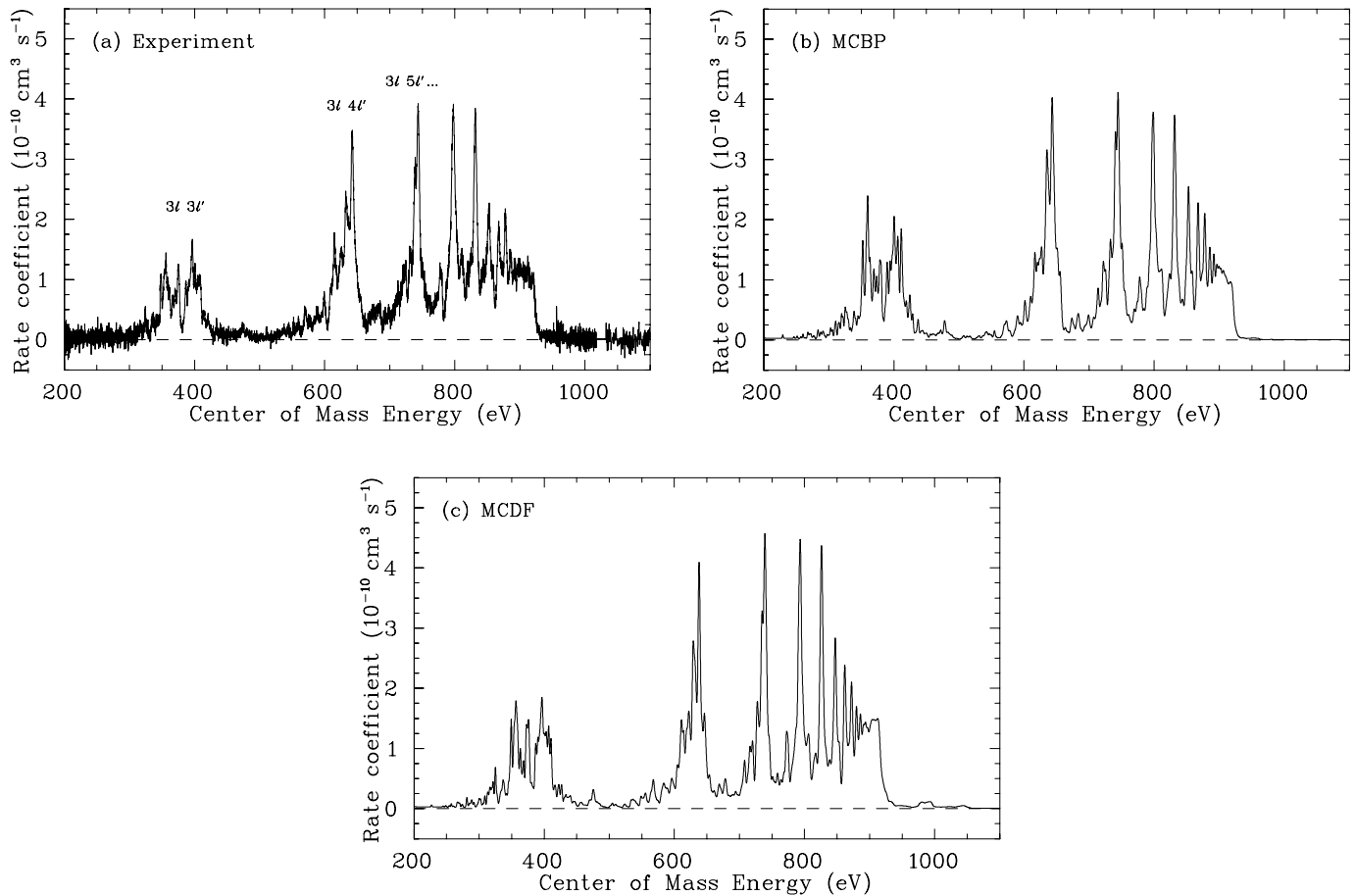
FIG. 2.—Fe XIX to Fe XVIII DR resonances due to $2 \rightarrow 3$ core excitations ($n_{max} = 130$): (*a*) experiment, (*b*) MCBP, and (*c*) MCDF. The experimental and theoretical data represent the DR cross section times the electron-ion relative velocity convolved with the energy spread of the experiment (the merged-beam rate coefficient $\langle \sigma v \rangle$). The data are shown vs. electron-ion collision energy. In (*a*) the measured DR resonances due to various $3lnl'$ doubly excited states are labeled. The small gap above 1000 eV is due to an accidental nonoverlap of measurement energy scans. The nonresonant RR " background " rate in (*b*) and (*c*) has been calculated using a modified semiclassical technique.

ward calculation is discussed in Savin (1999) and Savin et al. (1999).

We can also derive a $2 \rightarrow 3$ DR rate coefficient from our experimental results presented here. This Maxwellian-averaged rate is given by

$$\alpha(T_e) = \frac{2}{\sqrt{\pi k_B T_e}} \int_0^\infty \sqrt{\frac{E_{cm}}{k_B T_e}} e^{-E_{cm}/k_B T_e} \sigma(E_{cm}) v(E_{cm}) dE_{cm} .$$

(5)

Because the experimental energy spread is small compared to the measurement energies, v varies insignificantly over the energy range sampled at each measurement energy. Hence, we can accurately approximate σv in equation (5) using our measured $\langle \sigma v \rangle$.

Adding together our experimentally derived DR rate coefficients for $2 \rightarrow 2$ and $2 \rightarrow 3$ DR yields a Maxwellian-averaged rate coefficient that can be used for plasma modeling. Our experimentally derived rate coefficient is shown in Figure 3. We estimate that for $k_B T_e \geq 1$ eV, the uncertainty in the absolute magnitude of our experimental rate is $\lesssim 20\%$. Contributions due to DR into $n \geq n_{max} = 130$, which are not accessible in our setup, are calculated theoretically to increase the summed $2 \rightarrow 2$ and $2 \rightarrow 3$ DR rate coefficient by less than 3%. Our experimental rate coefficient

does not include contributions due to $1 \rightarrow 2$ DR. Our calculations indicate that the addition of the $1 \rightarrow 2$ channel would increase our DR rate coefficient by $\lesssim 1\%$ for $k_B T_e \leq 10,000$ eV.

Our experimental rate coefficient may include some weak contributions due to $2 \rightarrow 4$ DR. The $2 \rightarrow 4$ resonances are predicted to span a range in collision energy from ≈ 800 to 1200 eV. In the range 1000–1100 eV, these resonances are predicted to peak at a value of $\approx 2 \times 10^{-11}$ cm^3 s^{-1}. It is possible that while correcting the parabolic shape to the background (as described above), we may have slightly overcompensated and subtracted out some of the $2 \rightarrow 4$ resonances from our data, particularly in the 1000–1100 eV range. However, as is obvious from Figure 2, we see no significant resonance structure in this energy range. Based on our multiconfiguration Breit-Pauli results, we calculate that inclusion of the $2 \rightarrow 4$ channel increases the summed $1 \rightarrow 2$, $2 \rightarrow 2$, and $2 \rightarrow 3$ DR rate coefficients by $\lesssim 0.03\%$ for $k_B T_e = 100$ eV, 2.1% for 400 eV, 3.8% for 1000 eV, 5.0% for 4000 eV, and 5.3% for 10,000 eV. However, the lack of any discernible $2 \rightarrow 4$ structure in our measured data suggests that the strength of the $2 \rightarrow 4$ resonances is smaller than predicted and that their actual contribution to the total Maxwellian rate coefficient is smaller than the numbers quoted here.
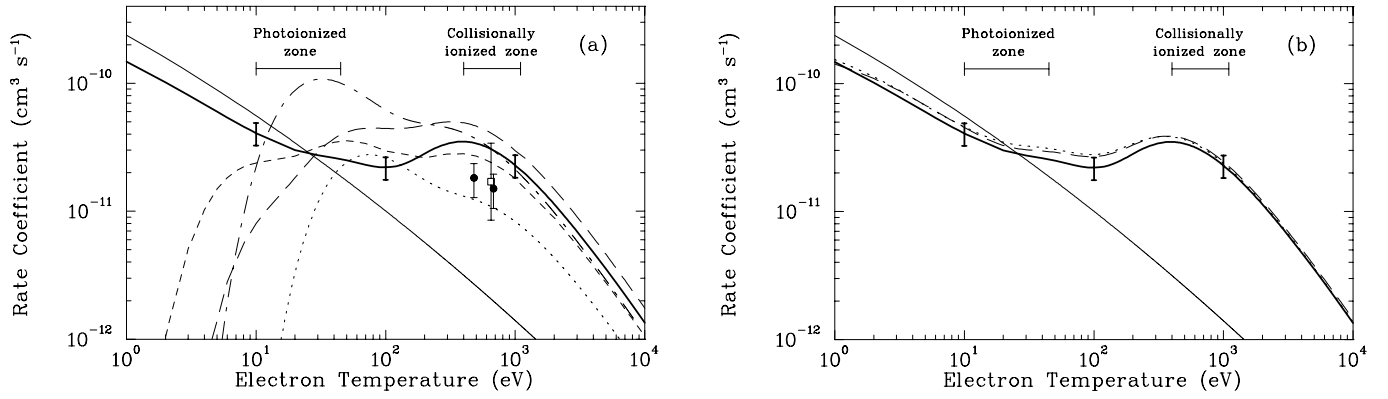
Fig. 3.—Fe XIX to Fe XVIII Maxwellian-averaged DR rate coefficient for recombination. (a) The thick solid curve represents our experimentally derived rate coefficient using our $2 \rightarrow 2$ and $2 \rightarrow 3$ results ($n_{max} = 130$). The thick error bars show our estimated total experimental uncertainty of $\lesssim 20\%$. The tokamak results are from Isler et al. (1982; filled circles) and Wang et al. (1988; open square). Also shown are the published theoretical DR rate coefficients of Jacobs et al. (1977) as fitted by Shull & van Steenberg (1982; dotted curve), of Roszman (1987; short-dashed curve), and of Dasgupta & Whitney (1994; long-dashed curve) as well as the recommended DR rate coefficient of Mazzotta et al. (1998; dot–long-dashed curve). As a reference we give the recommended RR rate coefficient of Arnaud & Raymond (1992; thin solid curve). (b) As in (a) the thick solid curve represents our experimentally derived rate coefficient and the thin solid curve the recommended RR rate. Also shown are our MCBP (dotted curve) and MCDF (dashed curve) DR results for $n_{max} = \infty$. Both calculations include DR via $1 \rightarrow 2$, $2 \rightarrow 2$, and $2 \rightarrow 3$ core excitations. None of the experimental or theoretical DR rate coefficients in (a) or (b) include RR.

The accuracy of our experimental DR rate coefficient for $k_B T_e < 1$ eV is difficult to assess. This is due to the difficulty of quantifying the uncertainty in the inferred, near 0 eV resonance strengths and energies. The contribution to the summed $2 \rightarrow 2$ and $2 \rightarrow 3$ experimental rate coefficient due to these inferred resonances is 100% for $k_B T_e \lesssim 0.01$ eV, 56% for 0.1 eV, 18% for 1 eV, and $\lesssim 2\%$ for $k_B T_e \gtrsim 10$ eV. These percentages also describe the contribution of the inferred resonances to the total $2 \rightarrow 2$ Maxwellian rate coefficient when compared with our results in Savin et al. (1999), which did not include these inferred resonances.

We have fitted our experimentally derived rate coefficient using the simple fitting formula

$$\alpha_{DR}(T_e) = T_e^{-3/2} \sum_i c_i e^{-E_i/k_B T_e}, \qquad (6)$$

where c_i is the resonance strength for the ith fitting component and E_i the corresponding energy parameter. Table 1 lists the best-fit values for the fit parameters. The fit is good to better than 0.7% for 0.001 eV $\leq k_B T_e \leq 10,000$ eV.

4. THEORY

Theoretical calculations of rate coefficients for DR onto Fe XIX have been carried out by Jacobs et al. (1977), Roszman (1987), and Dasgupta & Whitney (1994). The calculations of Jacobs et al. (1977) and Roszman (1987) were carried out in LS coupling using a single-configuration, nonrelativistic model. The calculations of Dasgupta & Whitney (1994) were carried out in intermediate coupling using a single-configuration, Hartree-Fock (HF) model with relativistic corrections. Details about these three calculations may be found in the cited references. Fits to the rates of Jacobs et al. (1977) are presented by Shull & van Steenberg (1982).

For comparison with our present experimental results, we have carried out new calculations using two independent state-of-the-art theoretical methods: multiconfiguration Breit-Pauli (MCBP) and multiconfiguration Dirac-Fock (MCDF). Here we briefly describe these techniques.

4.1. Multiconfiguration Breit-Pauli

DR cross section calculations are carried out with the code AUTOSTRUCTURE (Badnell 1986), which relies on lowest order perturbation theory and uses the isolated resonance, independent process approximation to compute Lorentzian resonance profiles. Our basic approach for highly charged Fe systems has been detailed more fully in Savin et al. (2002). Briefly, a bound orbital basis $\{1s, 2s, 2p, 3s,$

TABLE 1
FIT PARAMETERS

Parameter	Experiment	MCBP	MCDF
c_1	2.14E$-$5	1.94E$-$5	5.65E$-$6
c_2	1.05E$-$5	2.83E$-$5	7.28E$-$6
c_3	4.34E$-$5	2.52E$-$5	4.34E$-$5
c_4	6.62E$-$5	4.27E$-$4	2.67E$-$5
c_5	3.86E$-$4	1.25E$-$3	4.43E$-$4
c_6	1.24E$-$3	5.53E$-$3	1.38E$-$3
c_7	5.56E$-$3	4.50E$-$2	5.01E$-$3
c_8	4.07E$-$2	2.44E$-$1	4.88E$-$2
c_9	2.92E$-$1	1.51E0	3.10E$-$1
c_{10}	1.46E0	0.00E0	1.55E0
E_1	8.72E$-$3	6.01E$-$2	2.00E$-$3
E_2	2.11E$-$2	7.05E$-$2	8.57E$-$3
E_3	7.58E$-$2	2.22E$-$1	5.93E$-$2
E_4	6.49E$-$1	1.29E0	2.46E$-$1
E_5	1.66E0	4.91E0	1.33E0
E_6	5.82E0	2.21E1	5.19E0
E_7	2.50E1	8.66E1	2.25E1
E_8	9.59E1	3.30E2	9.24E1
E_9	4.01E2	7.46E2	3.67E2
E_{10}	7.88E2	0.00E0	7.86E2

NOTE.—For the experimentally derived rate coefficient for Fe XIX DR via the $N = 2 \rightarrow N' = 2$ and $N = 2 \rightarrow N' = 3$ core excitation channels ($n_{max} = 130$). Also given are the fit parameters for our calculated MCBP and MCDF results ($n_{max} = \infty$). The MCBP and MCDF data are for the sum of DR via $1 \rightarrow 2$, $2 \rightarrow 2$, and $2 \rightarrow 3$ core excitations. The units are cm^3 s^{-1} K$^{1.5}$ for c_i and eV for E_i.

$3p, 3d, 4s, 4p, 4d, 4f$} for the Fe^{18+} target states is generated by performing a configuration-averaged HF calculation (Froese-Fischer 1991) for the $1s^22s^22p^4$ state to get the first three orbitals, followed by a configuration-averaged, frozen-core HF calculation for the $1s^22s^22p^3nl$ states to get the additional $n = 3$ and $n = 4$ orbitals. Distorted wave calculations are then performed to generate the appropriate free ϵl and bound nl orbitals, which are attached to each target configuration to yield the Fe^{17+} continuum and resonance states, respectively. All of the above orbitals are computed in the absence of any relativistic effects. However, the continuum and resonance states are subsequently recoupled to an intermediate coupling scheme in order to include relativistic effects to lowest order.

Computation of the DR cross section has been broken up into separate $2 \rightarrow 2$, $2 \rightarrow 3$, $2 \rightarrow 4$, and $1 \rightarrow 2$ calculations as follows: First, for $2 \rightarrow 2$ DR, we include all possible $2l^6nl'$ resonance configurations, with $6 \leq n \leq 1000$ and $0 \leq l' \leq 15$, and all accessible $2l^6\epsilon l''$ continuum configurations. The Fe^{18+} target energies have been adjusted to the experimental values of Sugar & Corliss (1985). To account for field ionization effects, we also eliminated all resonances with $n > 130$.

For $2 \rightarrow 3$ DR, the resonance configurations included are given by $2l^53l'nl''$ with $3 \leq n \leq 1000$ and $0 \leq l'' \leq 6$. Contributions from higher l'' levels are unimportant because the $3 \rightarrow 2$ core radiative rate is much larger than for $2 \rightarrow 2$. This results in a greatly reduced capture rate for DR into these higher l'' levels. We note also that results for $3 \leq n \leq 35$ yielded results nearly identical to those using an upper limit of 1000 for n. The $2l^6\epsilon l'''$ continuum states used for $2 \rightarrow 2$ transitions now have to be augmented for $2 \rightarrow 3$ DR to include all accessible $2l^53l'\epsilon l'''$ configurations.

The $2 \rightarrow 4$ region becomes more difficult to treat than the $2 \rightarrow 3$ one since we now have a $4f$ core electron. Furthermore, the $2l^54l'nl''$ resonances (with $4 \leq n \leq 1000$ and $0 \leq l'' \leq 6$) can decay not only to all those continua considered above but also to the $2l^53l'\epsilon l'''$ continua. We included these additional resonances and continua, which lead to a calculation much more computationally intensive than for $2 \rightarrow 3$ DR.

Finally, in order to treat $1s \rightarrow 2p$ DR, we need to consider additional final channels due to core, or spectator, Auger decay. Inner shell-excited $1s2l^7nl''$ resonance states can decay not only to the $1s^22l^6\epsilon l'''$ continuum configurations but also to $1s^22l^5nl''\epsilon l''$ configurations, which we also include in our calculations. Because of the large $2 \rightarrow 1$ core radiative decay, we now need only to include resonance states for $2 \leq n \leq 35$ and $0 \leq l'' \leq 6$. No adjustment to the target energies was done for the $2 \rightarrow 3$, $2 \rightarrow 4$, or $1 \rightarrow 2$ DR calculations since these resonances lie well above the threshold and therefore give resonance strengths that are insensitive to small shifts in energies.

In Figure 2b we present the MCBP-calculated resonance structure for Fe XIX DR with $n_{max} = 130$. Figure 3b shows the resulting Maxwellian-averaged rate coefficient for DR via $1 \rightarrow 2$, $2 \rightarrow 2$, and $2 \rightarrow 3$ core excitations with $n_{max} = \infty$.

We have fitted our MCBP rate coefficient (for $n_{max} = \infty$) using equation (6). Table 1 lists the best-fit values for the fit parameters. The fit is good to better than 1.5% for $0.01 \leq k_B T_e \leq 10,000$ eV. For $k_B T_e < 0.01$ eV, the rate coefficient fit is only good to $\lesssim 30\%$, but since Fe XIX is predicted to form at $k_B T_e \gg 0.01$ eV and since the rate coeffi-

cient is rapidly going to zero in this range, the reliability of the fit below 0.01 eV is unimportant.

4.2. *Multiconfiguration Dirac-Fock*

DR cross sections and rate coefficients are calculated in the independent processes and isolated resonance approximations (Seaton & Storey 1976). In this framework, the DR cross section can be written as the product of the dielectronic capture cross section, which is just the inverse Auger cross section and the radiative branching ratio. The required transition energies and wave functions for the atomic states involved are evaluated using the MCDF method in intermediate coupling with configuration interaction from the same complex. The Auger and radiative transition rates are computed using the first-order perturbation theory and the MCDF model.

For $2 \rightarrow 2$ excitations, explicit calculations are carried out for $n \leq 30$ and $l \leq 12$ (for more details, see Savin et al. 1999). The resonance energies are adjusted by using the experimental excitation energies (Corliss & Sugar 1982). For the $2l$–$3l'$ excitations, detailed calculations are performed for autoionizing states with $3 \leq n \leq 15$ and $l \leq 6$. Since the contributions to the total DR rate coefficients from $n > 15$ are less than 8% for all temperatures, extrapolation from $n = 15$ would introduce no more than an estimated 1% error in the total DR rate coefficient. For $1s$–$2p$ excitations, we include only intermediate states with $n \leq 8$ and $l \leq 3$. No energy adjustment is applied to the $2l$–$3l'$ and $1s$–$2p$ excitations. The contributions from the high-n Rydberg states are taken into account using an n^{-3} scaling for the appropriate Auger and radiative rates. All possible Auger transitions and radiative transitions to bound states are included in the calculations of radiative branching ratios. A one-step cascade correction is employed when the main radiative decay leads to another autoionizing state.

In Figure 2c we present the MCDF calculated resonance structure for Fe XIX DR with $n_{max} = 130$. Figure 3b shows the resulting Maxwellian-averaged rate coefficient for DR via $1 \rightarrow 2$, $2 \rightarrow 2$, and $2 \rightarrow 3$ core excitations with $n_{max} = \infty$.

We have fitted our MCDF rate coefficient (for $n_{max} = \infty$) using equation (6). Table 1 lists the best-fit values for the fit parameters. The fit is good to better than 1.1% for 0.001 eV $\leq k_B T_e \leq 10,000$ eV.

5. DISCUSSION

Rate coefficients for DR onto Fe XIX have been inferred from tokamak measurements using time-dependent models of the line emission and ionization structure of the plasmas (Isler, Crume, & Arnurius 1982; Wang et al. 1988). We have plotted these inferred rate coefficients in Figure 3a. The tokamak results of Isler et al. (1982) are discrepant with our results. Part of the reason for this may be due to errors in the models used to infer their DR rate coefficients. The results of Wang et al. (1988) agree with our experimentally derived DR rate coefficient, to within their estimated factor of 2 error bars.

The results of Jacobs et al. (1977), Roszman (1987), and Dasgupta & Whitney (1994), as well as the recommended DR rate coefficient of Mazzotta et al. (1998), are also plotted in Figure 3a. These rate coefficients do not include DR contributions due to $2p_{1/2} \rightarrow 2p_{3/2}$ core excitations. Thus,

they do not reproduce the correct low-temperature behavior for the DR rate coefficient (Savin et al. 1999).

Fe XIX is predicted to peak in fractional abundance in an optically thin, photoionized plasma with cosmic abundances over the range $k_B T_e \approx 10$–45 eV (Kallman & Bautista 2001). Over this temperature range the rate coefficients of Jacobs et al. (1977), Roszman (1987), Dasgupta & Whitney (1994), and Mazzotta et al. (1998) can go from being in fortuitous agreement with our results to differing by orders of magnitude. The true temperature at which an ion forms in a photoionized plasma can vary depending on the metallicity of the gas, the shape of the ionizing spectrum, and additional heating and cooling mechanisms. Thus, for reliable models of photoionized plasmas, it is crucial that the low-temperature behavior of the DR rate coefficient be accurately known.

In electron-ionized plasmas an ion peaks in fractional abundance at a fixed temperature, as long as three-body recombination is unimportant. Fe XIX is predicted to peak in abundance in an electron-ionized plasma at $k_B T_e \approx 685$ eV (Mazzotta et al. 1998). At this temperature, the rate coefficient of Jacobs et al. (1977) is a factor of ≈ 3 smaller than our data, the results of Roszman (1987) are a factor of 1.18 times smaller, and those of Dasgupta & Whitney (1994) are a factor of 1.33 times larger. The rate coefficient of Mazzotta et al. (1998) is in fortuitously good agreement.

As demonstrated above and by Savin et al. (1999), a comparison of DR rate coefficients alone cannot be used reliably to benchmark different theoretical techniques. Theoretical rate coefficients can be in fortuitously good agreement with experiment. The most reliable method for verifying the accuracy of DR calculations is by a detailed comparison between experimental and theoretical resonance strengths and energies.

Figures 2a, 2b, and 2c show our experimental and theoretical results for DR of Fe XVIII via $2 \rightarrow 3$ core excitations. A visual comparison shows that experiment and theory are, in general, in good agreement. The theoretical and experimental resonance peak energies agree to within $\approx 1\%$. We take this agreement as an estimate for the accuracy of our E_{cm} calibration of the measurement.

To quantify the comparison between experiment and theory, in Table 2 we list the integrated resonance strengths, $\int_{E_{min}}^{E_{max}} \sigma_{DR} dE$, for selected limits of integration. We identify the dominant DR resonance complex for each energy range, list the integrated experimental and theoretical resonance

strengths, and give the ratio of the theoretical results to the experimental results. The most significant discrepancies occur for the $3l3l'$ resonances. The MCBP and MCDF results are, respectively, $\approx 47\%$ and $\approx 31\%$ larger than experiment. These differences are larger than the total experimental uncertainty, which is estimated to be less than 20%. Finally, the small difference between the results of the two calculations above 950 eV is due to the omission of one-step radiative cascades by the MCBP calculation, which is accounted for in the MCDF calculation. This difference has an insignificant effect on the total DR rate coefficient.

In Figure 4 we present a more detailed view of the experimental and theoretical results for the $3l3l'$ resonances. Although we see reasonable agreement between theory and experiment in the overall resonance structure, there are still some significant differences in the detailed structure and magnitude of the resonances. To investigate these discrepancies, we carried out several more MCBP calculations. First, we looked at the effect of determining the $n = 3$ HF orbitals from the $3l3l'$ configurations rather than the singly excited states. This produced little change in our MCBP results. We then carried out an MCBP calculation using orbitals determined from a Slater-type orbital model potential. The peak at 360 eV showed some sensitivity to the change of atomic structure—a reduction in height to 2×10^{-10}. Finally, we included the mass-velocity and Darwin terms in the solution of the radial equations rather than treating them as a perturbation on the Hamiltonian. This resulted in a lowering of peak positions by ≈ 5 eV, but overall, we could not obtain significantly improved agreement with experiment.

6. CONCLUSIONS

We have measured DR resonance strengths and energies for Fe XIX forming Fe XVIII due to $2 \rightarrow 2$ and $2 \rightarrow 3$ core excitations. We have also calculated the relevant DR data using the perturbative MCBP and MCDF methods. We find good agreement between theory and experiment except for a few of the $2 \rightarrow 2$ DR resonances as reported in Savin et al. (1999) and for the $3l3l'$ DR resonances, as reported here.

Using our measured resonance strengths and energies, we have produced a Maxwellian-averaged rate coefficient for use in plasma modeling. Our MCBP and MCDF rate coefficients are in good agreement with our experimentally derived results. Previously published rate coefficients are in

TABLE 2
INTEGRATED RESONANCE STRENGTHS

COMPLEX	E_{min} (eV)	E_{max} (eV)	$\int_{E_{min}}^{E_{max}} \sigma_{DR} dE$ (cm^2 eV)			RATIO	
			Exp.	MCBP	MCDF	MCBP/Exp.	MCDF/Exp.
$3l3l'$	200	500	6.24E−18	9.17E−18	8.17E−18	1.47	1.31
$3l4l'$	500	665	6.57E−18	6.71E−18	6.73E−18	1.02	1.02
$3l5l'$	665	765	5.60E−18	5.26E−18	5.37E−18	0.938	0.957
$3l6l'$	765	805	3.23E−18	2.89E−18	3.45E−18	0.897	1.07
$3l7l'$	805	838	2.96E−18	2.62E−18	2.69−18	0.885	0.909
$3lnl'$ ($n \geq 8$)	838	1017	6.09E−18	5.68E−18	6.64E−18	0.933	1.09

NOTE.—For selected energy ranges of the $2 \rightarrow 3$ DR resonances shown in Figs. 2a–2c. Listed are the dominant resonance complex for each energy range, the limits of integration E_{min} and E_{max}, the integrated experimental, MCBP, and MCDF resonance strengths, and the ratio of the MCBP and MCDF results to the experimental results. The RR background has been subtracted from all data sets.
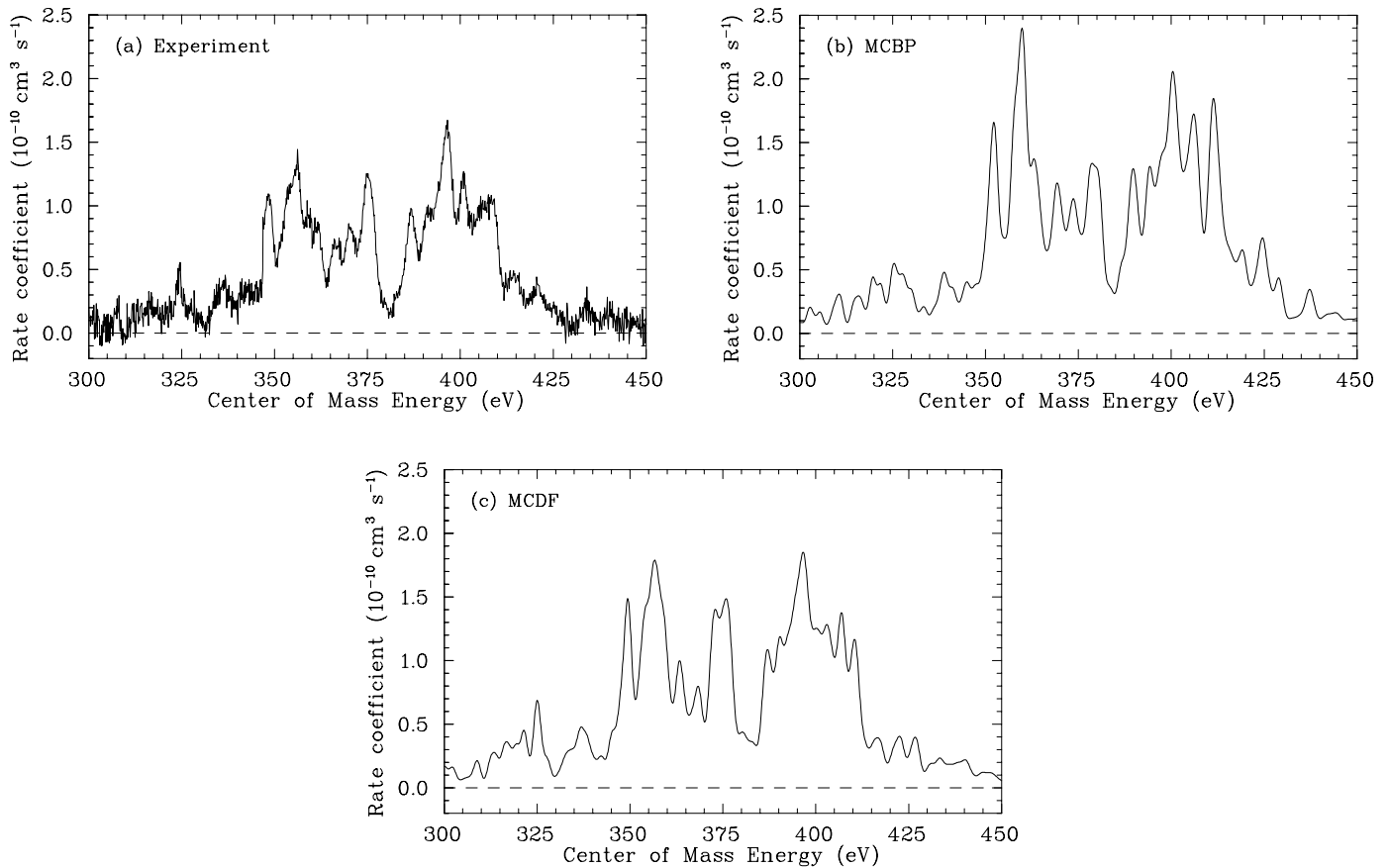
Fig. 4.—Fe XIX to Fe XVIII $3l3l'$ resonances due to DR via $2 \rightarrow 3$ core excitations: (*a*) experiment, (*b*) MCBP, and (*c*) MCDF. See Fig. 2 for details.

poor agreement, none of which reliably reproduce the magnitude or the temperature dependence of the DR rate coefficient.

The uncertainty in the DR rate coefficients for oxygen-like ions forming fluorine-like ions is one of the limiting factors for reliably interpreting solar and stellar upper atmosphere observations (Savin & Laming 2002). We have used our measurements to benchmark two independent, state-of-the-art perturbative techniques (the MCBP and MCDF methods) for calculating DR of oxygen-like ions. It should now be possible to use either of these two techniques with a high degree of reliability to calculate DR for other ions along the oxygen isoelectronic sequence. This will help to improve our understanding of the solar and stellar upper atmosphere observations.

REFERENCES

Arnaud, M., & Raymond, J. 1992, ApJ, 398, 394
Badnell, N. R. 1986, J. Phys. B, 19, 3827
Brickhouse, N. S., Raymond, J. C., & Smith, B. W. 1995, ApJS, 97, 551
Brinkman, A. C., et al. 2000, ApJ, 530, L111
Cheng, K. T., Kim, Y.-K., & Desclaux, J. P. 1979, At. Data Nucl. Data Tables, 24, 111
Corliss, C., & Sugar, J. 1982, J. Phys. Chem. Ref. Data, 11, 135
Dasgupta, A., & Whitney, K. G. 1994, At. Data Nucl. Data Tables, 58, 77
Doschek, G. A., & Cowan, R. D. 1984, ApJS, 56, 67
Dupree, A. K., Brickhouse, N. S., Doschek, G. A., Green, J. C., & Raymond, J. C. 1993, ApJ, 418, L41
Ferland, G. J., Korista, K. T., Verner, D. A., Ferguson, J. W., Kingdon, J. B., & Verner, E. M. 1998, PASP, 110, 761

Froese-Fischer, C. 1991, Comput. Phys. Commun., 64, 369
Gwinner, G., et al. 2000, Phys. Rev. Lett., 84, 4822
———. 2001, Phys. Scr., T92, 319
Hoffknecht, A., et al. 1998, J. Phys. B, 31, 2415
Hoffknecht, A., Schippers, S., Müller, A., Gwinner, G., Schwalm, D., & Wolf, A. 2001, Phys. Scr., T92, 402
Isler, R. C., Crume, E. C., & Arnurius, D. E. 1982, Phys. Rev. A, 26, 2105
Jacobs, V. L., Davis, J., Keeple, P. C., & Blaha, M. 1977, ApJ, 211, 605
Kallman, T. R., & Bautista, M. 2001, ApJS, 133, 221
Kaspi, S., Brandt, W. N., Netzer, H., Sambruna, R., Chartas, G., Garmire, G. P., & Nousek, J. A. 2000, ApJ, 535, L17
Kilgus, G., Habs, D., Schwalm, D., Wolf, A., Badnell, N. R., & Müller, A. 1992, Phys. Rev. A, 46, 5730

Lampert, A., Wolf, A., Habs, D., Kilgus, G., Schwalm, D., Pindzola, M. S., & Badnell, N. R. 1996, Phys. Rev. A, 53, 1413
Linkemann, J., et al. 1995, Nucl. Instrum. Methods Phys. Res., B98, 154
Lum, K. S. K., et al. 1992, ApJS, 78, 423
Mazzotta, P., Mazzitelli, G., Colafrancesco, S., & Vittorio, N. 1998, A&AS, 133, 403
Mewe, R. 1991, A&A Rev., 3, 127
Mewe, R., Gronenschild, E. H. B. M., & van den Oord, G. H. J. 1985, A&AS, 62, 197
Müller, A. 1999, Int. J. Mass Spectrom., 192, 9
Müller, A., & Wolf, A. 1997, in Accelerator-Based Atomic Physics Techniques and Applications, ed. S. M. Shafroth & J. C. Austin (New York: AIP), 147
Roszman, L. J. 1987, Phys. Rev. A, 35, 3368
Savin, D. W. 1999, ApJ, 523, 855
———. 2000, ApJ, 533, 106
Savin, D. W., et al. 1997, ApJ, 489, L115

Savin, D. W., et al. 1999, ApJS, 123, 687
———. 2000, in Proceedings of the 12th APS Topical Conference on Atomic Processes in Plasmas, ed. R. C. Mancini (New York: AIP), 267
———. 2002, ApJS, 138, 337
Savin, D. W., & Laming, J. M. 2002, ApJ, 566, 1166
Schippers, S., Bartsch, T., Brandau, C., Gwinner, G., Linkemann, J., Müller, A., Saghiri, A. A., & Wolf, A. 1998, J. Phys. B, 31, 4873
Schippers, S., Bartsch, T., Brandau, C., Müller, A., Gwinner, G., Wissler, G., Beutelspacher, M., Grieser, G., & Wolf, A. 2000, Phys. Rev. A, 62, 022708
Schippers, S., et al. 2001, ApJ, 555, 1027
Seaton, M. J., & Storey, P. J. 1976, in Atomic Processes and Applications, ed. P. G. Burke & B. L. Moisewitch (Amsterdam: North-Holland), 133
Shull, J. M., & van Steenberg, M. 1982, ApJS, 48, 95 (erratum 49, 351)
Sugar, J., & Corliss, C. 1985, J. Phys. Chem. Ref. Data, 14, 2
Wang, J.-S., Griem, H. R., Hess, R., & Rowan, W. L. 1988, Phys. Rev. A, 38, 4761